Design and Analysis of a 2-DOF Split-Stator Induction Motor

Jikai Si, Haichao Feng, Liwang Ai, Yihua Hu, *Member, IEEE*, and Wenping Cao, *Senior Member, IEEE*

***Abstract*—A two degrees of freedom (2-DOF) actuator capable of producing linear translation, rotary motion, or helical motion would be a desirable asset to the fields of machine tools, robotics, and various apparatuses. In this paper, a novel 2-DOF split-stator induction motor was proposed and electromagnetic structure parameters of the motor were designed and optimized. The feature of the direct-drive 2-DOF induction motor lies in its solid mover arrangement. In order to study the complex distribution of the eddy current field on the ferromagnetic cylinder mover and the motor's operating characteristics, the mathematical model of the proposed motor was established, and characteristics of the motor were analyzed by adopting the permeation depth method (PDM) and finite element method (FEM). The analytical and numerical results from motor simulation clearly show a correlation between the PDM and FEM models. This may be considered as a fair justification for the proposed machine and design tools.**

***Index Terms*—Finite element method (FEM), induction motor, permeation depth method (PDM), solid rotor, split stator, two degrees of freedom (2-DOF).**

I. Introduction

THE DRIVE mechanism with a two degrees of freedom (2-DOF) driver capable of generating linear, rotary or helical motions has extensive applications in the manufactures of mechanical tools such as robots for chip production lines, robotic arms, injection machines, and boring machines [1]–[4]. Traditionally, the realization of 2-DOF driving technologies is achieved by two or more rotary electrical motors and complicated middle mechanical motion converters. Currently, the state-of-the-art 2-DOF drivers have the advantages of high mechanical integration and reliability, which also save the intricate mechanical transmission in the middle of the drive devices.

[1]–[4] proposed some permanent magnet (PM) rotary-linear motors with twin-armature stators. The structure of these motors is similar to the coaxial series structure with PM tubular linear motor and rotary motor, which has the advantages of easy manufacturing, low cost, but suffers from a short axial stroke and a large volume. [5]–[7] put forward PM and induction rotary-linear motors with twin-windings. The common feature of them is that their cores are embedded with two orthogonal windings: a rotary winding and a linear winding. Because of the direction of the stator laminations, the eddy current of one direction can be suppressed while that of the other direction can be serious.

As for the 2-DOF induction motors, their movers are commonly of solid ferromagnetic cylinder structure. [8] adopted a field-circuit coupling method to calculate parameters of the solid rotor. [9] analyzed the eddy current field and the efficiency of a solid rotor induction motor based on electromagnetic field calculations. [10]–[12] studied the equivalent circuit parameters of a solid rotor induction motor. [13] and [14] analyzed the operational characteristics of a solid rotor induction motor by using an analytical diffusion equation in the complex domain. [15]–[17] used the finite element method (FEM) to study the performance of a solid rotor asynchronous motor. [18] focused on the additional loss of a solid rotor induction motor by using a two-dimensional (2-D) numerical method. [19] studied the influence of slotting on the rotor loss of a solid rotor induction motor. It can be seen that these structures are characterized with high mechanical robustness and simplicity, high reliability and controllability, and low manufacturing and maintenance costs. However, the consequent eddy current field on the ferromagnetic cylinder mover affects the performance of the motor but is extremely difficult to analyze with accuracy.

This paper proposes a novel topology of a 2-DOF split-stator induction motor. Its electromagnetic parameters are calculated and optimized by three rounds of sequential single-variable optimization. The rotor parameter of the rotary part is calculated by using the permeation depth method (PDM). Then the equivalent circuit model can be obtained and its characteristics are investigated based on the single-phase equivalent circuit. A 2-D numerical model of the proposed motor is built in the finite element software *MagNet* to compare with the analytical results. The results obtained from analyzing and calculating of the rotary part can be applied to the linear part because of the equivalence between the rotary and linear motions. Thus, only the rotary part of the motor is analyzed in the following sections.

II. Structure and Principles of Operation

A. Basic Structure

The proposed 2-DOF induction motor is shown in Fig. 1. It consists of two arc-shaped half-stators: 1) one for rotary motion; and 2) one for linear motion. The half stator for rotary motion is of the semicircle annular shape, and is composed of a stator

Manuscript received May 5, 2014; revised November 29, 2014; accepted March 20, 2015. This work was supported by the National Natural Science Foundation of China under Grant 51277054 and Grant U1361109, and the Project for Henan Polytechnic University Middle-Young Age Top-Notch Innovative Personnel HPUSEEA-001. Paper no. TEC-00304-2014.

J. Si, H. Feng, and L. Ai are with School of Electrical Engineering and Automation, Henan Polytechnic University, Jiaozuo 45400, China (e-mail: sijikai527@126.com; fhc@hpu.edu.cn; ailiwang1009@163.com).

Y. Hu is with the Department of Electronic and Electrical Engineering, University of Strathclyde, Glasgow G11XQ, U.K. (e-mail: yihua.hu@strath.ac.uk).

W. Cao is with the School of Electronics, Electrical Engineering, and Computer Science, Queen's University, Belfast BT9 5AH, U.K. (e-mail: w.cao@qub.ac.uk).

Color versions of one or more of the figures in this paper are available online at http://ieeexplore.ieee.org.

Digital Object Identifier 10.1109/TEC.2015.2418578

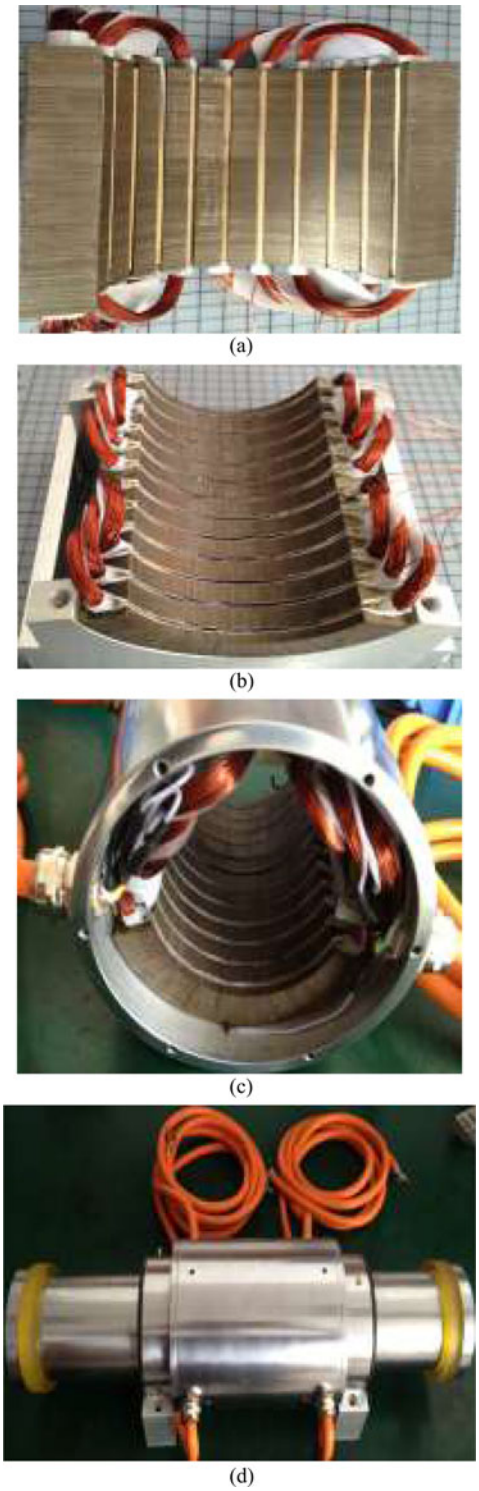

Fig. 1. Proposed 2-DOF induction motor. (a) Stator for rotary motion. (b) Stator for linear motion. (c) Stator of the 2-DOF induction motor. (d) Assembly of the 2-DOF induction motor.

core slotted along the axial direction. The half stator for linear motion consists of an arc-shaped stator core slotted along the circumferential direction. The two half-stators are assembled into a whole stator and share a secondary cylinder mover coated with conductive sheets.

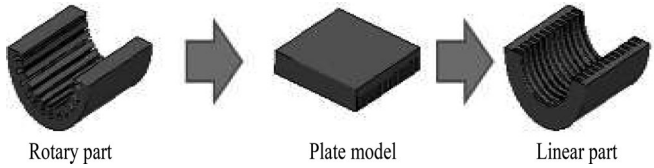

Fig. 2. Equivalent transformation.

TABLE I
MAIN DESIGN PARAMETERS OF THE 2-DOF INDUCTION MOTOR

Parameter	Rotary part	Linear part
Rated power (P_N)	1.1 kW	1.1 kW
Rated voltage (U_N)	220 V (Y)	220 V (Y)
Frequency (f)	50 Hz	25 Hz
Pole pair (p)	2	2
Stator inner diameter	98 mm	98 mm
Stator outer diameter	155 mm	155 mm
Stator axial length	135 mm	156 mm
Air-gap thickness	2 mm	2 mm
Slot number	12	12
Number of turns of the coil	65	65
Axial length of the mover	655 mm	655 mm

B. Principles of Operation

When the motor is supplied with three-phase ac power, the half-stator for rotary motion can generate a rotating magnetic field. Due to the electromagnetic induction, an axial eddy-current field will be induced in the mover and an electromagnetic force on the mover will be generated. This in turn generates a rotary torque. Similarly, the other half-stator can generate a traveling magnetic field and a circumferential current on the surface of the mover. The induced electromotive force will move the mover in an axial direction. By controlling the power of two sets of stator windings, the proposed motor is capable of producing rotary, linear or helical motions.

III. PRELIMINARY DESIGN AND OPTIMIZATION

A. Determination of Electromagnetic Parameters

If the interaction between the rotary and linear motions is neglected, the machine could be regarded as two separate parts. The transformation between the rotary part and linear part should balance the radial force caused by two half-stators of the motor, as shown in Fig. 2. A complete rotary motor ($P_N = 2.2\ kW, p = 4, U_N = 220\ V, f = 50\ Hz$) is first designed following the traditional design process. A half of it is taken as the rotary part of the 2-DOF induction motor and the parameters of the linear part are obtained via equivalent transformation. The main design parameters of the motor are listed in Table I, the slot shapes are shown in Fig. 3 and the geometric parameters of the slots are given in Table II.

B. Influence of the Air-Gap Thickness

After obtaining the parameters for the rotary part, the finite element model with the mover coated with two conductive sheets

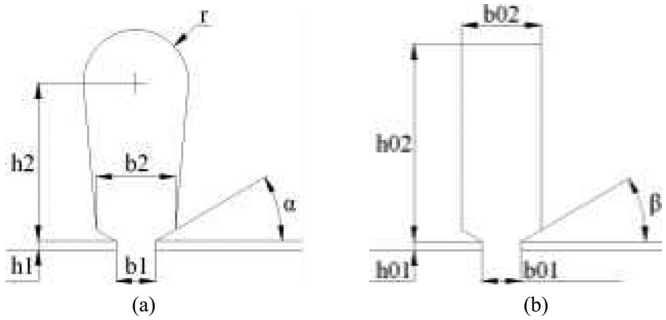

Fig. 3. Slot shape of the two half-stators. (a) For rotary motion. (b) For linear motion.

TABLE II
DIMENSIONS OF THE STATOR SLOT

Linear motion		Rotary motion	
$b1$	2.8 mm	$b0$	2.8 mm
$b2$	7.7 mm	$b02$	9.5 mm
$h1$	0.5 mm	$h01$	0.5 mm
$h2$	18.5 mm	$h02$	22.3 mm
α	30°	β	30°
r	5.1 mm		

is established, as shown in Fig. 4. The load torque is set to 6 Nm while the air-gap thickness changes from 0.5 to 5 mm at the interval of 0.5 mm, in order to investigate the influence of the air gap thickness on the motor performance. At a given air-gap value, the average speed and torque, speed fluctuation magnitude and torque fluctuation, and the rotor power loss are calculated under a steady-state operation. Simulation results are presented in Fig. 5 for comparison.

It can be seen that the average speed increases initially and then decreases with the increase of the air-gap thickness and the maximum speed is attained at the air-gap thickness of 2.5–3 mm. In essence, the greater the air-gap is, the smaller the speed fluctuation is. The torque fluctuation and total rotor loss generally decrease as the air-gap thickness increases. The air-gap thickness is different when the average speed, the speed fluctuation magnitude, torque fluctuation magnitude and total rotor loss reach their maximum, the overall performance is excellent for the 3-mm air-gap. Therefore, this is used in the design.

C. Influence of the Rotor Material

The rotor is constructed with a cylindrical stack of silicon-iron laminations surrounded by a conductive cylindrical sleeve, which in turn may be divided in two conductive layers. In the finite element model with a 6-Nm load torque, the total thickness of the conductive layer is 2 mm (1 mm each for the two layers). A series of simulation with different rotor materials (ferromagnetic, steel, aluminum, copper, steel-aluminum and steel-copper composite) are conducted and compared in terms of the average speed, speed fluctuation magnitude, torque fluctuation magnitude, and the total rotor loss. These are presented in Fig. 6.

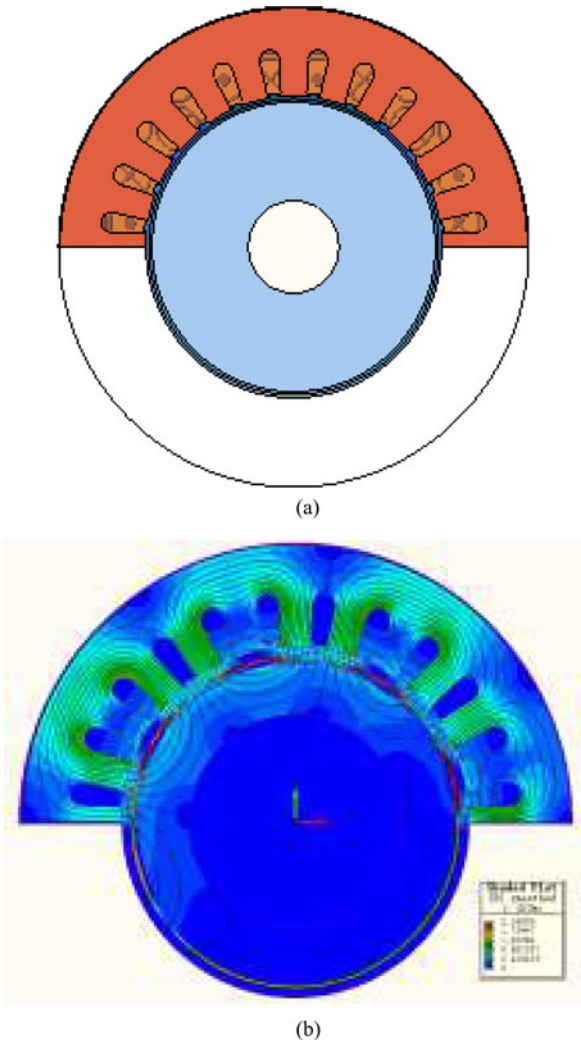

Fig. 4. FEM model of the rotary part. (a) FEM model. (b) Distribution of flux density.

From Fig. 6, it can be seen that steel-copper composite is a good option to strike a balance the speed fluctuation magnitude, torque fluctuation magnitude rotor power loss and average speed. Therefore, it is selected for the rotor material. So the conductive layer is determined to be a steel-copper composite structure (out layer is steel and inner layer is copper).

D. Influence of the Conductor Layer Thickness

Likewise, 0.5 –5 mm at a step of 0.5 mm are chosen to examine the influence of the conductor layer thickness. The average speed, speed fluctuation magnitude and torque fluctuation magnitude as well as the rotor power loss are obtained for a given layer thickness. The results are plotted in Fig. 7.

These results show that the average speed reaches its maximum while the speed fluctuation magnitude and torque fluctuation magnitude as well as the rotor loss are relatively low when

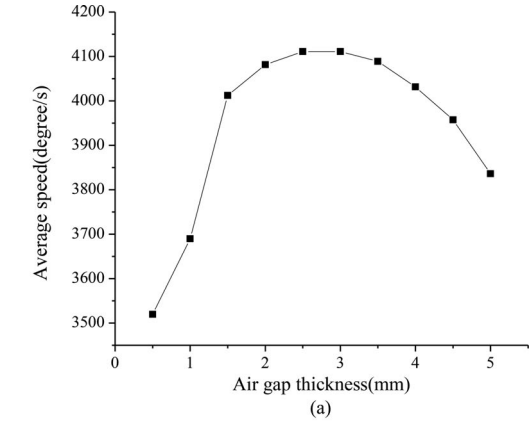

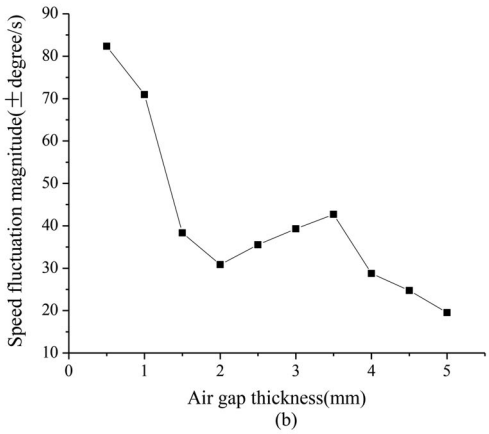

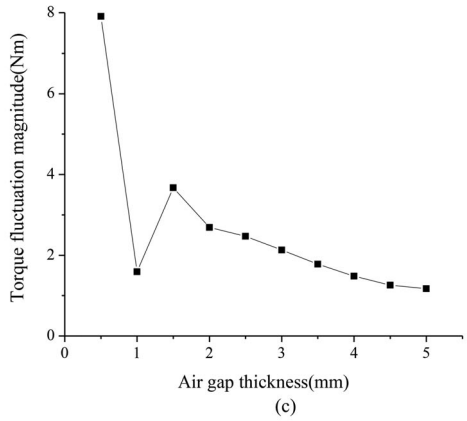

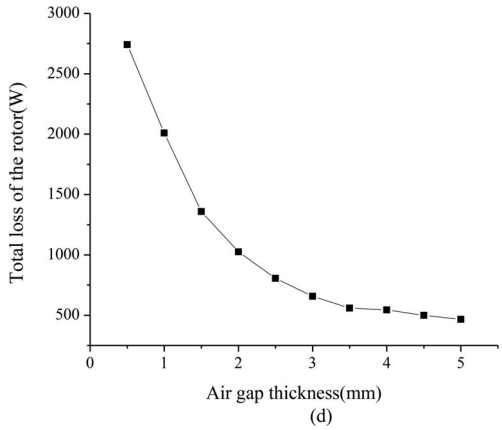

Fig. 5. Optimization of the air-gap thickness. (a) Average speed. (b) Speed fluctuation magnitude. (c) Torque fluctuation magnitude. (d) Rotor power loss.

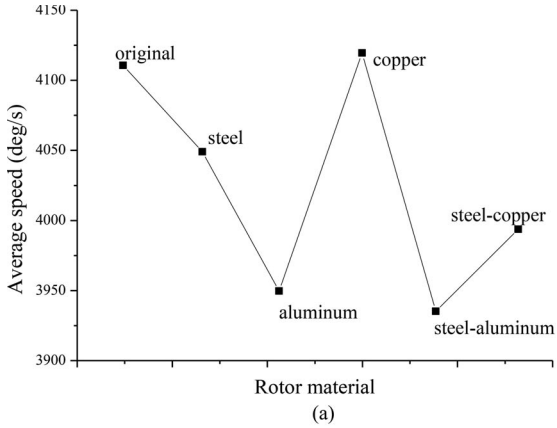

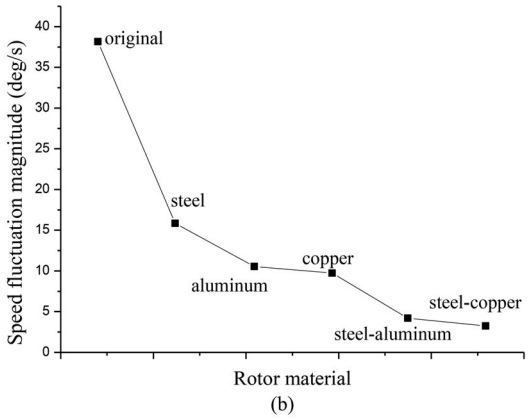

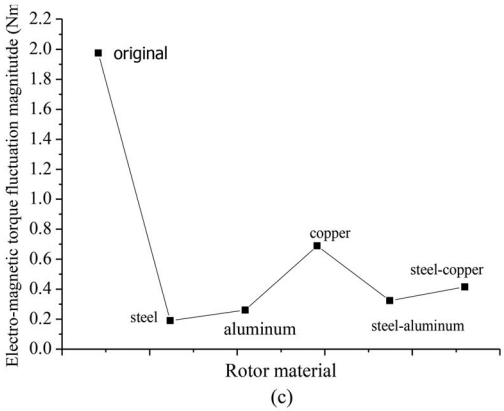

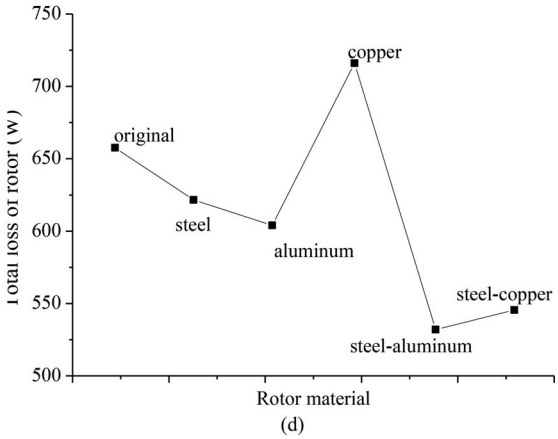

Fig. 6. Choice of the rotor material. (a) Average speed. (b) Speed fluctuation magnitude. (c) Torque fluctuation magnitude. (d) Rotor power loss.

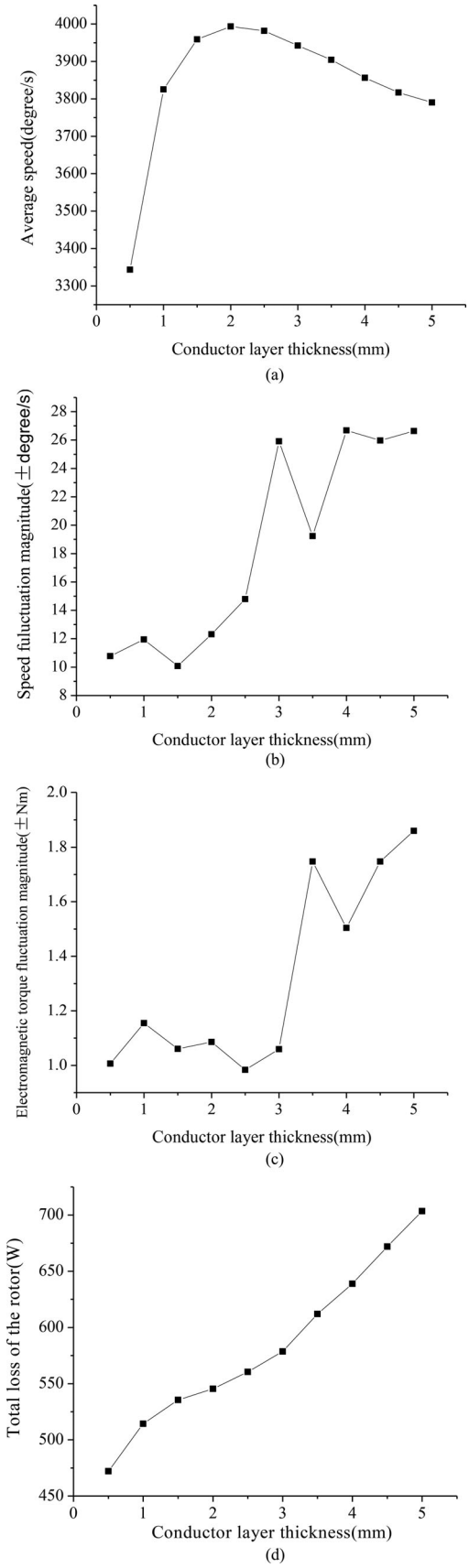

Fig. 7. Optimization of the conductor layer thickness. (a) Average speed. (b) Speed fluctuation magnitude. (c) Torque fluctuation magnitude. (d) Total rotor loss.

the conductor layer thickness is 2 mm. Therefore, this is chosen as the conductor layer thickness.

IV. Theoretical Analysis

The mover of the proposed motor adopting a ferromagnetic cylindrical structure has both complicated magnetic circuits and electrical circuits. In practice, the rotor current and magnetic fluxes tend to converge toward the surface of the conducting material owing to the skin effect. The eddy current field and main magnetic field are clearly different to the traditional three-phase induction motors. In this regard, the PDM may be a good analytical method to study the characteristics of induction motors with solid rotors. This is achieved by analyzing and calculating the rotor parameters after referring to a normal *T*-shape equivalent circuit. The rationale of the PDM is the expansion of the rotor into a semi-infinite plane, which is suitable for linear parts. Due to the damping effect, the electromagnetic field suffers from attenuation after penetrating into the rotor. For simplicity of the analysis, this study defines the following assumptions.

1) The longitudinal end effect is neglected.
2) The rotor is seen as a semi-infinite ferromagnetic plane.
3) The eddy current is distributed in an ultra-thin area with the width of $0.5\pi D_2$, thickness Δ, and length L.
4) In the axial direction, the eddy current density is uniform. In the radial direction, the eddy current density is distributed as a sine wave in the period of 2τ.

Then the rotor resistance per phase is calculated by

$$r_2 = \rho \frac{L}{A} \tag{1}$$

where ρ is the resistivity of the rotor material; L is the length of the coupling part of the stator and the rotor; A is the total cross-sectional area passed by the eddy current, which is computed by

$$A = 0.5\pi D_2 \Delta \tag{2}$$

whereD_2 is the rotor outer diameter; Δ is the depth of penetration, which is given by

$$\Delta = \sqrt{\frac{2}{\omega \sigma \mu_2}} = \sqrt{\frac{2\rho}{s\omega_1 \mu_0 \mu_1}} \tag{3}$$

where μ_0 is the air permeability; μ_1 is relative permeability of the rotor material; ω_1 is the angular frequency of the stator supply. Then the rotor phase resistance referred to the stator system is

$$r_2' = \frac{mN_1^2 K_{\mathrm{dp1}}^2}{s} \rho \frac{L}{\pi D_2 \Delta} K_r K_e K_1 \tag{4}$$

whereN_1 is the effective number of turns per phase for stator winding. K_{dp1} is the stator winding factor. $K_r \approx 1.45$ takes into account the nonlinear magnetic permeability and hysteresis losses for the resistance. The coefficient $K_x \approx 0.85$ takes into account the nonlinear magnetic permeability and hysteresis losses for the reactance. K_e is the end-effect correction factor and K_1 is the curvature effect correction factor.

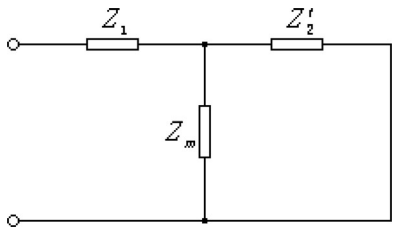

Fig. 8. *T*-equivalent circuit of induction motors.

Considering the cylindrical structure of the rotor, the saddleback distribution of the air-gap field caused by the finite length of the rotor and the existence of magnetic hysteretic loss, the calculated value of the rotor is updated to the actual value adopting all kinds of correction factors obtained by previous research [9].

According to the characteristic that the impedance angle of ferromagnetic material is constant [9], [12], x_2' and Z_2' can be obtained from r_2'.

$$x_2' = \frac{m_1 N_1 K_{\mathrm{dp1}}^2}{s} \rho \frac{L}{\pi D_2 \Delta} K_x K_e K_1 \tag{5}$$

$$Z_2' = r_2' + j x_2'. \tag{6}$$

By neglecting the longitudinal end effect, Z_2 of the rotor can be referred to the stator as Z_2' in the *T* equivalent circuit, as shown in Fig. 8. Z_1 can be easily calculated as in traditional induction motors.

However, the above analysis is based on the lock-rotor condition (i.e., the slip is unity). The proposed motor is similar to conventional induction motors in that the rotor resistance in the equivalent circuit is a function of slip; but is dissimilar in that its impedance angle of the solid ferromagnetic rotor is constant. Therefore, there is a settled relationship between the equivalent resistance and reactance of the rotor. The rotor reactance and impedance are given by

$$\begin{cases} r_{2s}' = \frac{r_2'}{s} \\ x_{2s}' = \frac{x_2'}{s} \\ Z_{2s}' = \frac{Z_2'}{s} \end{cases} \tag{7}$$

where r_2', x_2', Z_2' are the rotor parameters when the motor is standstill. The tangential magnetic density and relative permeability of the rotor surface, depth of penetration and rotor reactance can be obtained at a given slip. By changing the slip between 0.1 and 1, the permanence depth and rotor impedance are calculated and plotted in Fig. 9.

As the slip increases, the skin effect on the rotor circuit becomes more severe, increasing the likelihood of saturation and the difficulty of field penetration. This is observed in Fig. 9(a) that the depth of penetration decreases with the slip. Furthermore, the reactance and impedance have similar trends as the slip increases owing to the constant impedance angle of the rotor, as is shown in Fig. 9(b).

According to the *T*-equivalent circuit shown in Fig. 8, some characteristics of the motor can be calculated as traditional induction motors. This paper adopts the PDM

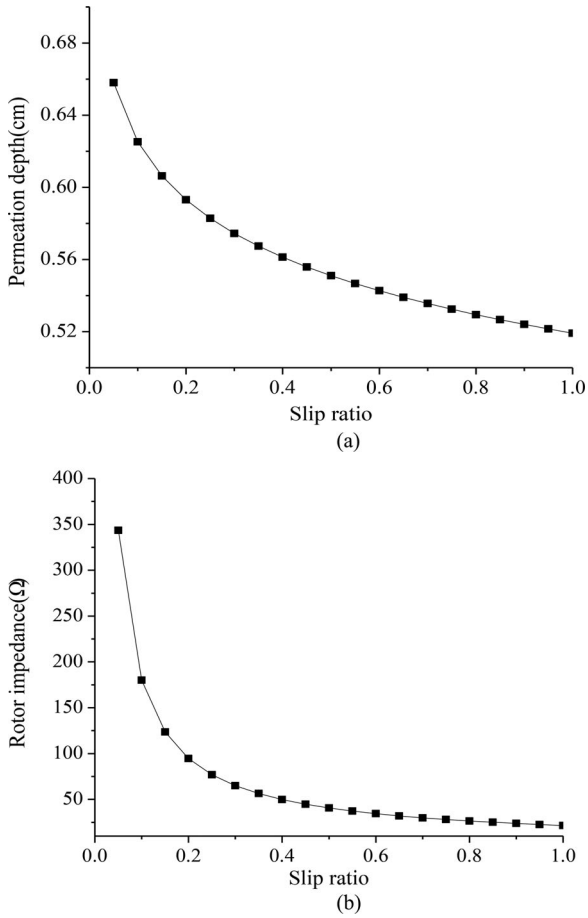

Fig. 9. Rotor parameter as a function of the slip. (a) Permeation depth. (b) Rotor impedance.

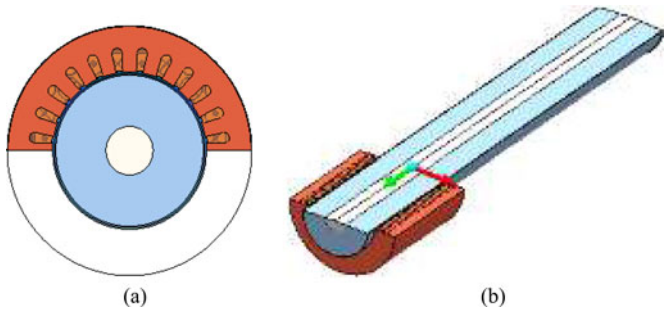

Fig. 10. FEM models. (a) Rotary part. (b) Linear part.

analysis and calculates the rotary part of the proposed induction motor. The analytical results are also suitable for analyzing the linear part after equivalent conversion as per the PDM.

V. Finite Element Simulation Analysis

A numerical model of the motor is established by using finite element software *MagNet*, as shown in Fig. 10. Main parameters of the electromagnetic field are solved by simulating the model and plotting the intuitive visual graphics of the magnetic field, current, torque/force and other parameters. The rotary motion

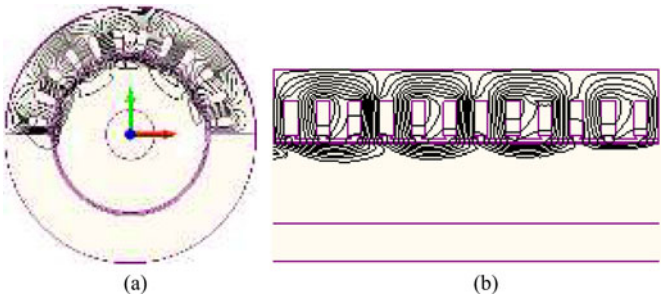

Fig. 11. Flux line distribution at $s = 0.05$. (a) Rotary part. (b) Linear part.

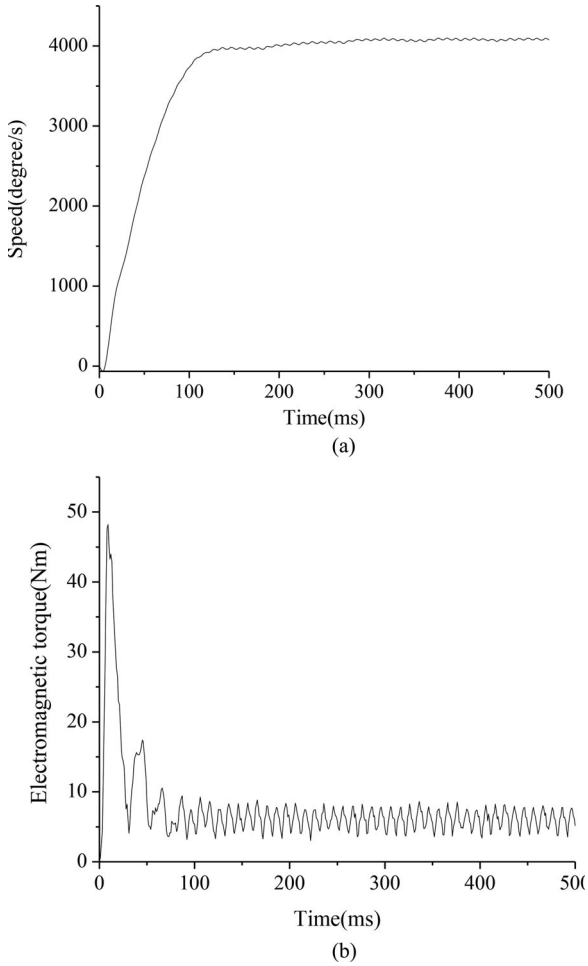

Fig. 12. Speed and torque of the rotary part. (a) Speed curve. (b) Electromagnetic torque curve.

stator and linear motion stator are fed by three-phase alternating voltage source ($U_N = 220$ V, $f = 50$ Hz) and ($U_N = 220$ V, $f = 25$ Hz), respectively. Fig. 11 (a)–(b) shows the flux line distribution of the rotary and linear parts, respectively. Fig. 12 shows the speed and electromagnetic torque of the rotary part when a load torque of 6 Nm is applied. Fig. 13 presents the peed and electromagnetic force of the linear part when a load force of 120 N is applied.

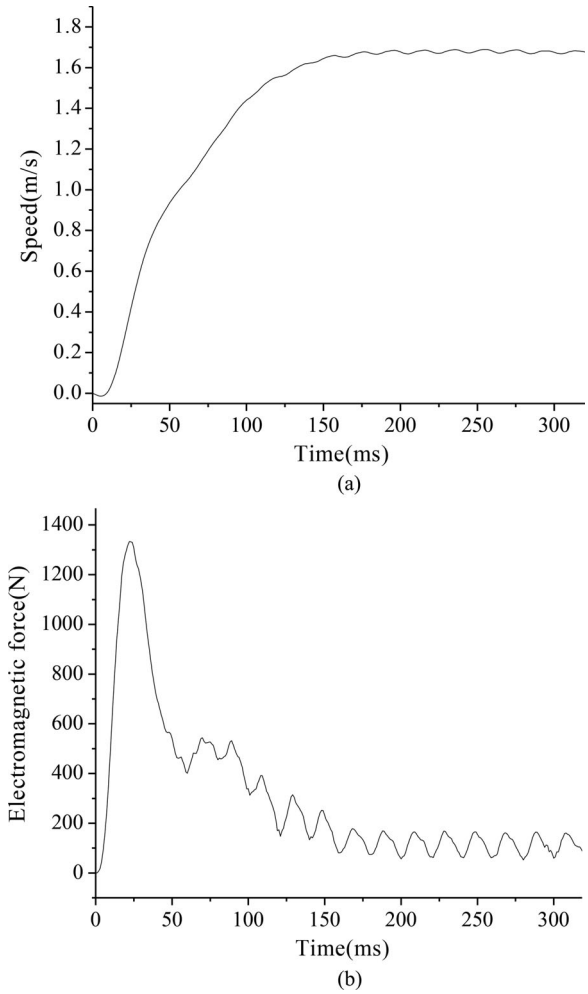

Fig. 13. Speed and force of the linear part. (a) Speed curve. (b) Electromagnetic force curve.

VI. Results Analysis and Discussion

The electromagnetic design and analysis are conducted for the rotary part with 50-Hz supply frequency, and the linear part with 25-Hz supply frequency. Analytical and numerical results are compared between PDM and FEM in terms of the electromagnetic torque, stator phase current, power factor and efficiency as presented in Fig. 14.

From Fig. 14, electromagnetic torque, stator current and power factor increase with slip while the efficiency initially increases and then decreases passing its maximum point. Numerical and analytical results agree well with one another for the torque and power factor whilst there are some differences in the stator current and efficiency. These may arise from computation errors in PDM due to the following reasons.

1) The default rotor current only flows in the deep end of the slot when adopting the PDM.
2) The tangential component of the magnetic field is only taken into account when calculating the magnetic field on the rotor surface.
3) The choice of correction factors is empirical, depending on the experience of the motor designer.

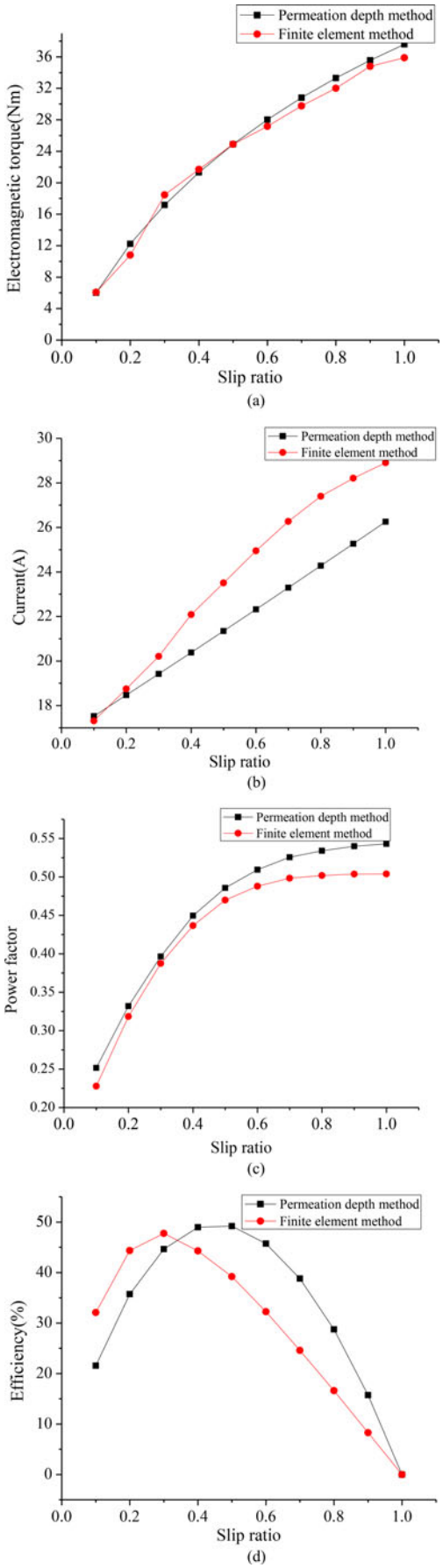

Fig. 14. FEM and PDM results for comparison. (a) Electromagnetic torque. (b) Stator phase current. (c) Power factor. (d) Efficiency.

VII. Conclusion

This paper has presented a novel split-stator 2-DOF induction motor. The analytical and numerical models have been established to analyze the motor performance adopting the PDM and FEM methods. The following conclusions are obtained.

1) The electromagnetic structural parameters of the induction motor are preliminarily designed and the key parameters impacting on the motor performance are examined and optimized including the air-gap thickness, rotor material, and the thickness of the mover conductive layer.
2) The analytical model of the rotary part was established by the PDM but it is difficult to predict the motor characteristics because of the complex eddy current field.
3) By comparing analytical and numerical results from PDM and FEM, the feasibility of applying the PDM is confirmed.

The future work will investigate the dual magnetic fields of the proposed motor and establish a three-dimensional model to analyze the mutual effect of the 2-DOF motions. In addition, an experimental test rig with control circuits will be developed to carry out experimental validation.

References

[1] K. J. Meessen, J. J. H. Paulides, and E. A. Lomonova, "Analysis and design considerations of a 2-DoF rotary-linear actuator," in *Proc. IEEE Int. Elect. Mach. Drives Conf.*, 2011, pp. 336–341.
[2] P. Bolognesi, "A novel rotary-linear permanent magnets synchronous machine using common active parts," in *Proc. 15th IEEE Mediterranean Electrotech. Conf.*, 2010, pp. 1179–1183.
[3] P. Bolognesi and F. Papini, "FEM modeling and analysis of a novel rotary-linear isotropic brushless machine," in *Proc. Conf. Elect. Mach.*, 2011, pp. 1–6.
[4] P. Bolognesi, "Structure and theoretical analysis of a novel rotary-linear isotropic brushless machine," in *Proc. Int. Conf. Elect. Mach.*, 2010, pp. 1–6.
[5] K. J. Meessen, J. J. H. Paulides, and E. A. Lomonova, "Analysis of a novel magnetization pattern for 2-DoF rotary-linear actuators," *IEEE Trans. Magn.*, vol. 48, no. 11, pp. 3867–3870, Nov. 2012.
[6] E. A. Mendrela and E. Gierczak, "Double-winding rotary-linear induction motor," *IEEE Trans. Energy Convers.*, vol. EC-2, no. 1, pp. 47–54, Mar. 1987.
[7] J. Fleszar and E. A. Mendrela, "Twin-armature rotary-linear induction motor," *IEE Proc. B*, vol. 130, no. 3, pp. 186–192, Mar. 1983.
[8] C. Liu and R. Yao, "A coupled field-circuit approach to the calculation for parameters of solid rotor induction machine," *J. Shanghai Jiaotong Univ.*, vol. 37, no. 9. pp. 1372–1374, Sep. 2003.
[9] Z. Chang, "Electro-magnetic calculation of induction motor with composite rotor," M.S. thesis, Key Lab. Aviation Power, Nanjing Univ. Aeronautics Astronautics, Nanjing, China, Feb. 2007.
[10] C. Liu and R. Yao, "A new approach to calculate equivalent circuit parameters of the induction motor with solid rotor," in *Proc. Elect. Mach. Drives Conf.*, 2003, pp. 1612–1615.
[11] I. A. M. Abdel-Halim, "Approximate equivalent circuit for small solid-rotor induction motors," *IEE Proc. B Elect. Power. Appl.*, vol. 131, no. 2, pp. 70–72, Nov. 1984.
[12] L. T. Ergene and S. J. Salon, "Determining the equivalent circuit parameters of canned solid-rotor induction motors," *IEEE Trans. Magn.* vol. 41, no. 7, pp. 2281–2286, Jul. 2005.
[13] M. Markovic and Y. Perriard, "An analytical solution for the torque and power of a solid-rotor induction motor," in *Proc. Elect. Mach. Drives Conf.*, 2011, pp. 1053–1057.
[14] M. Mirzayee, H. Mehrjerdi, and I. Tsurkerman, "Analysis of a high-speed solid rotor induction motor using coupled analytical method and reluctance networks," in *Proc. IEEE Int. Conf. Wireless Commun. Appl. Comput. Electromagn.*, 2005, pp. 537–540.
[15] S. L. Ho, S. Niu, and W. N. Fu, "A novel solid-rotor induction motor with skewed slits in radial and axial directions and its performance analysis using finite element method," *IEEE Trans. Appl. Supercond.*, vol. 20, no. 3, pp. 1089–1092, Jun. 2010.

[16] T. Yang, L. Zhou, and W. Jiang, "Calculation of eddy current losses in a solid-rotor cage induction motor by finite element analysis," in *Proc. Int. Conf. Elect. Mach. Syst.*, 2008, pp. 3656–3659.
[17] R. Ibtiouen, R. Kechroud, and O. Touhami, "Complex finite element analysis of a solid rotor induction motor," in *Proc. Elect. Mach. Drives Conf.*, 2003, pp. 449–453.
[18] Z. Chang, W. Huang, Y. Hu, and L. Liu, "Research on stray loss of smooth surface solid rotor induction motor based on 2D analytical approach," *Proc. CSEE*, vol. 27, no. 21, pp. 83–88, 2007.
[19] Y. Gessese, A. Binder, and B. Funieru, "Analysis of the effect of radial rotor surface grooves on rotor losses of high speed solid rotor induction motor," in *Proc. Int. Symp. Power Electron. Elect. Drives Autom. Motion*, 2010, pp. 1762–1767.

Jikai Si was born in China, in 1973. He received the B.S. degree in electrical engineering and automation from the Jiaozuo Institute of Technology, Jiaozuo, China, in 1998; the M.S. degree in electrical engineering from Henan Polytechnic University, Jiaozuo, China, in 2005; and the Ph.D. degree in 2008 from the School of Information and Electrical Engineering, China University of Mining and Technology, Xuzhou, China, in 2008.

His main research interests include the theory, application, and control of special motor.

Dr. Si is a Member of the Institute of Linear Electric Machine and Drives, Henan Province, China.

Haichao Feng was born in China, in 1983. He received the B.S. and M.S. degrees in electrical engineering and automation, control theory, and control engineering from the School of Electrical Engineering and Automation, Henan Polytechnic University, Jiaozuo, China, in 2005 and 2008, respectively.

He is a Teacher at the School of Electrical Engineering and Automation, Henan Polytechnic University. In recent years, he has participated in eight provincial and three country research projects, and has published more than eight academic papers. His research interests include the optimization design of linear and rotary machines, power electronics, and their controls.

Mr. Feng is a Member of the Institute of Linear Electric Machine and Drives, Henan Province, China.

Liwang Ai was born in China, in 1989. He received the B.S. degree in electrical engineering and automation from the Wanfang College of Science and Technology, Jiaozuo, China, in 2012, and the M.S. degree in electrical engineering from Henan Polytechnic University, Jiaozuo, China, in 2015.

His main research interests include the optimization design of linear and rotary machines, and the theory and application of special motor.

Yihua Hu (M'13) received the B.S. degree in electrical motor drives, and the Ph.D. degree in power electronics and drives from the China University of Mining and Technology, Jiangsu, China, in 2003 and 2011, respectively.

Between 2011 and 2013, he was with the College of Electrical Engineering, Zhejiang University, Hangzhou, China, as a Postdoctoral Fellow. Between November 2012 and February 2013, he was an Academic Visiting Scholar at the School of Electrical and Electronic Engineering, Newcastle University, Newcastle upon Tyne, U.K. He is currently a Research Associate in the Department of Electronic and Electrical Engineering, University of Strathclyde, Glasgow, U.K. He has published more than 50 technical papers in leading journals and conference proceedings. His research interests include photovoltaic generation systems, power electronics converters, and electrical motor drives.

Wenping Cao (M'05–SM'11) received the B.Eng. degree in electrical engineering from Beijing Jiaotong University, Beijing, China, in 1991, and the Ph.D. degree in electrical machines and drives from the University of Nottingham, Nottingham, U.K., in 2004.

He is currently a Senior Lecturer at Queen's University Belfast, Belfast, U.K. His research interests include the thermal performance of electric machines, drives, and power electronics.

Dr. Cao was the recipient of the Best Paper Award at the 9th Symposium on Linear Drives for Industry Application (LDIA'2013) Conference. He serves as an Associate Editor for the IEEE TRANSACTIONS ON INDUSTRY APPLICATIONS, *IET Power Electronics*, and nine other international journals. He is also a Member of the Institution of Engineering and Technology and a Fellow of the Higher Education Academy.